

Forced 3D reconnection in an exponentially separating magnetic field

David N. Hosking,^{1,2,*} Ian G. Abel,³ and Steven C. Cowley⁴

¹*Princeton Center for Theoretical Science, Princeton, NJ 08540, USA*

²*Gonville & Caius College, Trinity Street, Cambridge, CB2 1TA, UK*

³*Institute for Research in Electronics and Applied Physics,
University of Maryland, College Park, MD 20742, USA*

⁴*Princeton Plasma Physics Laboratory, Princeton, NJ 08540, USA*

(Dated: December 3, 2024)

We present a solvable scenario for 3D reconnection in a sheared magnetic field. We consider a localized external force that is applied slowly and then maintained, generating an Alfvénic perturbation that spreads along the field lines. Separation of the sheared field lines causes the scale of the perturbation across the field to decrease, enabling magnetic diffusion to be enhanced. For a fusion-motivated equilibrium with exponential field-line separation, we find a reconnection timescale proportional to $\mathcal{S}/\ln \mathcal{S}$ under magnetohydrodynamics (MHD) and to $\mathcal{S}^{1/3}$ for semi-collisional electron-only reconnection, where \mathcal{S} is the Lundquist number of the perturbed flux tube. We generalize these results to arbitrary magnetic geometries, showing that the latter is geometry-independent. Interestingly, we find that slower field-line separation yields an increased reconnection rate in MHD.

Introduction. The rate of magnetic reconnection—i.e., of topological reconfiguration of a magnetic field in a conducting medium—in a fully three-dimensional geometry is an issue of great significance both for fusion devices and for magnetized astrophysical systems. In this Letter, we present a solvable scenario for the 3D resistive reconnection of separating field lines. We consider a force applied locally to a narrow, sheared flux tube, inducing a resistively damped Alfvén-wave packet that thins as it propagates. Because the packet is associated with a change to the local magnetic-field direction, its resistive diffusion modifies the connectivity of the global field.

We focus primarily on a particular fusion-motivated equilibrium [Eq. (2)] with field lines that separate exponentially with distance [Fig. 1(a)]. It has been suggested, and is perhaps intuitively compelling, that the rate of reconnection of exponentially separating field lines is fast, i.e., at most logarithmic in the Lundquist number \mathcal{S} (the ratio of the ideal to nominal resistive timescales) [1, 2]. Indeed, naïvely, it seems intuitive that reconnection induced by a diffusive Alfvén wave, as described above, would be fast in this case: the wave would be sheared to resistive scales in $\ln \mathcal{S}$ Alfvén timescales. However, we find that the reconnection timescale remains proportional to a finite power of \mathcal{S} (see abstract). At the end of the Letter, we generalize to other geometries, finding *faster* reconnection for field lines that separate more slowly.

Clebsch coordinates. We represent the equilibrium magnetic field \mathbf{B}_0 with Clebsch coordinates ψ and α , i.e., $\mathbf{B}_0 = \nabla\psi \times \nabla\alpha$. We take ψ to have units of magnetic flux and α to be dimensionless. The Clebsch coordinates are constant along unperturbed field lines and so can be used to label them; the arc length ℓ along the line completes the coordinate set. The distance perpendicular to \mathbf{B}_0 between the field lines (ψ, α) and $(\psi + d\psi, \alpha)$ is

$$dl_{\perp} = \frac{|\nabla\alpha|}{B_0} d\psi. \quad (1)$$

The rate of separation of field lines on a surface of constant α (“ α surface”) is therefore encoded in the dependence of $|\nabla\alpha|$ on ℓ . This dependence will set the rate of magnetic reconnection in our calculation.

Model equilibrium. We shall consider as a model magnetic geometry the field of two wires, located at $x = \pm a$ and $y = 0$, each carrying current I_0 in the z direction. We embed this configuration in a uniform external field $B_{\text{ext}}\hat{z}$, so that, with $r^2 = x^2 + y^2$ and c the speed of light,

$$\mathbf{B}_0 = B_{\text{ext}}\hat{z} + \hat{z} \times \frac{\nabla\psi}{a}, \quad \psi = \frac{aI_0}{c} \ln [(r^2 + a^2)^2 - 4a^2x^2]. \quad (2)$$

The equilibrium (2) is visualized in Fig. 1(a). Toroidicity notwithstanding, each lobe resembles the magnetic field of a tokamak in a divertor configuration (with the lobes taken together, it resembles a “doublet” [3]). We expect the results of our Letter to be applicable to reconnection in such a device, forced, for example, by an ELM-control coil (whose effect on the topology of edge fields and transport may be crucial for sustained confinement [4–6]).

We consider specifically reconnection in the vicinity of the field line passing through the point $(-\sqrt{2}a, 0, 0)$ on the separatrix. As we show in Section 1 of the Supplementary Information, we may define α surfaces such that

$$|\nabla\alpha|^2 = \frac{\ell_0^2}{2a^4} \cosh\left(\frac{2z}{\ell_0}\right) + \frac{2a^2}{\ell_0^2} + \frac{36(z/\ell_0)^2}{\cosh(2z/\ell_0)} \quad (3)$$

on this field line, where $\ell(z)$ is the solution of

$$\frac{d\ell}{dz} = \frac{B_0}{B_{\text{ext}}} = \sqrt{1 + \frac{2a^2}{\ell_0^2 \cosh(2z/\ell_0)}}, \quad (4)$$

$\ell_0 = a^2 B_{\text{ext}}/4I_0$ is the magnetic-shear length (we take $\ell_0 = a$ in all numerical results presented in this Letter) and $B_0(\ell) = |\mathbf{B}_0|$. According to Eqs. (1) and (3), field lines separate exponentially with ℓ as $\ell \rightarrow \infty$.

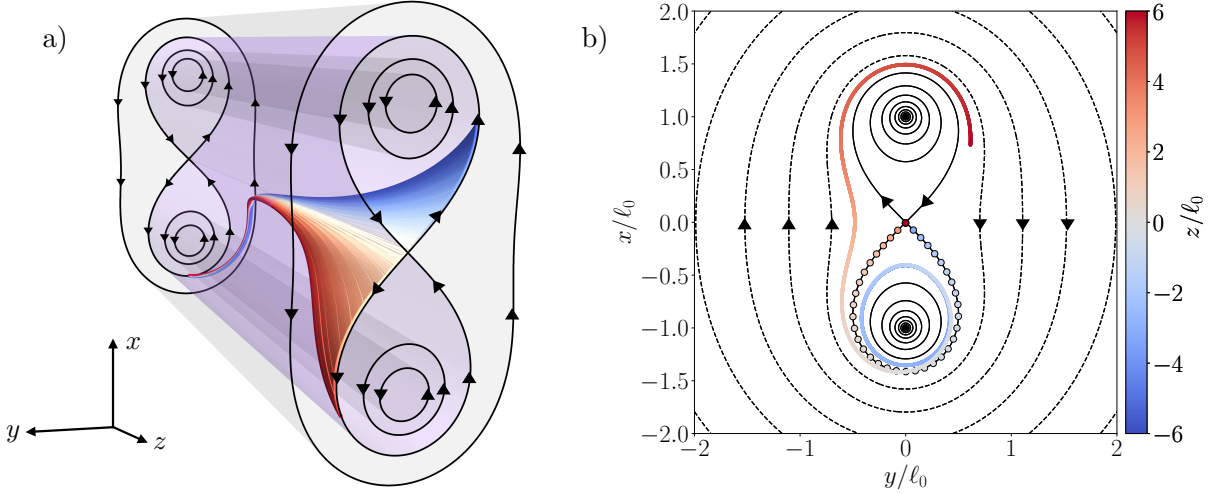


FIG. 1. Panel (a): The magnetic geometry considered in this study [Eq. (2)]. The surface of constant α along which we consider displacing a field line is shown with ψ increasing from blue to red. Arrows show the projection of the magnetic-field direction onto the xy -plane. Panel (b): Projection onto the xy -plane of the field line through $(-\sqrt{2}a, 0, 0)$ at (i) $\tilde{t} = 0$ (dots with black outlines) and (ii) $\tilde{t} \gg \tau_{\text{rec}}$ (blue-red line). Note that the orientation of the y -axis in panel (b) is different than in panel (a).

Dynamical model. We take the equilibrium magnetic field to be strong, and therefore consider a perturbation that is extended along the field line. We consider two dynamical regimes: the *MHD case*, in which the perpendicular scale of the perturbation is much larger than the ion gyroradius ρ_i , and the *kinetic case*, in which it is much smaller than ρ_i . The dynamical equations that we employ are those of low- β reduced MHD [7] in the MHD case and the semi-collisional limit of the Kinetic Reduced Electron Heating Model (KREHM) of Ref. [8] in the kinetic case. The latter regime is interesting *a priori* because the parallel group velocity of *kinetic* Alfvén waves is an increasing function of their perpendicular wavenumber [9]: the equilibrium shear causes them to accelerate and thus reach diffusive scales more quickly [10].

We assume an eikonal form for the velocity streamfunction Φ and perturbed magnetic-flux function Ψ , viz., $\Phi(\psi, \alpha, \ell, t) = \bar{\Phi}(\ell, t)e^{in\alpha}$ and $\Psi(\psi, \alpha, \ell, t) = \bar{\Psi}(\ell, t)e^{in\alpha}$, where $n \gg 1$ (cf. Refs. [11–14]). As we explain in Section 2 of the Supplementary Information, this choice yields

$$\left(\begin{array}{c} |\tilde{\nabla}\alpha|^2 \quad (\text{MHD}) \\ 1 \quad (\text{kinetic}) \end{array} \right) \times \frac{1}{\tilde{B}_0(\tilde{\ell})^2} \frac{\partial \tilde{u}}{\partial \tilde{t}} = \frac{\partial \tilde{J}_{\parallel}}{\partial \tilde{\ell}} + \tilde{F}(\tilde{\ell}, \tilde{t}), \quad (5)$$

and

$$\frac{1}{|\tilde{\nabla}\alpha|^2} \frac{\partial \tilde{J}_{\parallel}}{\partial \tilde{t}} = \frac{1}{\tilde{B}_0(\tilde{\ell})} \frac{\partial [\tilde{B}_0(\tilde{\ell})\tilde{u}]}{\partial \tilde{\ell}} - \frac{\tilde{J}_{\parallel}}{\mathcal{S}}. \quad (6)$$

The variables that appear in Eqs. (5) and (6) are as follows. The velocity in the α surface is $\delta \mathbf{u}_{\perp} = \mathbf{b}_0 \times \nabla \Phi = u(\psi, \alpha, \ell, t)e^{in\alpha} \mathbf{b}_0 \times \nabla \alpha$; $\delta \mathbf{B}_{\perp} = \mathbf{b}_0 \times \nabla \Psi = \delta B_{\perp}(\psi, \alpha, \ell, t)B_0(\ell)e^{in\alpha} \mathbf{b}_0 \times \nabla \alpha$ is the magnetic-field perturbation in the same surface; $\mathbf{b}_0(\ell) = \mathbf{B}_0/B_0$; and $J_{\parallel} = |\nabla \alpha|^2 \delta B_{\perp}$ is the perturbed

parallel current. Tildes signify normalization to the dimensionally appropriate combination of the shear length ℓ_0 and the ideal timescale τ_A . The latter is the shear-length crossing time of, in the MHD case, an Alfvén wave (i.e., $\tau_A = \ell_0/v_{A,\text{ext}}$, with $v_{A,\text{ext}}$ the Alfvén speed associated with B_{ext}) or, in the kinetic case, a kinetic Alfvén wave (i.e., $\tau_A = \sqrt{2}\ell_0^2/n\rho_i v_{A,\text{ext}}$). Similarly normalized, $\tilde{F}(\tilde{\ell}, \tilde{t})$ represents a force with the same eikonal dependence on α as Φ and Ψ , which pushes the field line along the α surface. We take \tilde{F} to have odd parity in $\tilde{\ell}$ and to turn on smoothly on the (normalized) timescale $\epsilon^{-1} \gg 1$, reaching a constant value at $\tilde{t} \gg \epsilon^{-1}$. In the numerical results shown in Figs. 1(b), 2 and 3, we choose $\tilde{B}_0(\tilde{\ell})^2 \tilde{F}(\tilde{\ell}, \tilde{t}) = \tilde{\ell}^3 e^{-\tilde{\ell}^2} (1 - e^{-\epsilon^2 \tilde{t}^2})$, absorbing the amplitude of \tilde{F} into the definitions of \tilde{u} , $\delta \tilde{B}_{\perp}$ and \tilde{J}_{\parallel} . The Lundquist number for the perturbed flux tube, \mathcal{S} , is

$$\mathcal{S} = \begin{cases} S/n^2 \sim 10^4 (100/n)^2 & (\text{MHD}) \\ \rho_{\star} S / \sqrt{2} n \sim 10^4 (100/n) & (\text{kinetic}) \end{cases} \quad (7)$$

where $S = v_{A,\text{ext}} \ell_0 / \eta$ is the Lundquist number of the global equilibrium, η is the magnetic diffusivity and $\rho_{\star} \equiv \rho_i / \ell_0$ is the normalized ion gyroradius. The numerical values quoted in Eq. (7) correspond to $\mathcal{S} \sim 10^8$ and $\rho_{\star} \sim 10^{-2}$, which are typical for a tokamak.

Eqs. (5) and (6) are linear in \tilde{u} and \tilde{J}_{\parallel} even though we have not required their amplitudes to be small compared with their perpendicular wavelengths. In this sense, the solutions we derive are valid nonlinearly [15].

Reconnected flux. Eq. (6) admits an invariant in the “ideal” limit $\mathcal{S} \rightarrow \infty$, given by

$$\Delta \psi = \int_{-\infty}^{\infty} d\tilde{\ell} \frac{\tilde{B}_0(\tilde{\ell})}{|\tilde{\nabla}\alpha|^2} \tilde{J}_{\parallel} = \int_{-\infty}^{\infty} d\tilde{\ell} \tilde{B}_0(\tilde{\ell}) \delta \tilde{B}_{\perp}. \quad (8)$$

$\Delta\psi$ is the difference (“step”) in the coordinate ψ of the perturbed field line between $\ell = -\infty$ and $\ell = +\infty$: $\Delta\psi \neq 0$ implies reconnection of field lines from inside the separatrix with those outside it [see Fig. 1(b)]. In a fusion device, this would cause the loss of confinement of hot plasma from inside the separatrix by streaming. Our goal is to determine the evolution of $\Delta\psi$ for finite $\mathcal{S} \gg 1$.

Late-time diffusive solutions. We consider the late-time ($\epsilon\tilde{t} \gg 1$) evolution of a diffusively spreading pulse induced by the force \tilde{F} . We plot numerical solutions of Eqs. (5) and (6) in Fig. 2. We now determine these solutions and their reconnection rates [Fig. 3] analytically.

We decompose the solutions into two regions: an inner region, where $\ell \sim \ell_0$ and the fluid inertia [left-hand side of Eq. (5)] can be neglected (because $\epsilon \ll 1$), and an outer region, where diffusion [last term in Eq. (6)] dominates over induction [first term in Eq. (6)].

MHD case: (i) Inner region (ideal). Neglecting inertia, Eq. (5) yields

$$\tilde{J}_{\parallel\text{in}}(\tilde{\ell}, \tilde{t}) = - \int_{-\infty}^{\tilde{\ell}} d\tilde{\ell}' \tilde{F} + \tilde{J}_{\parallel 0}(\tilde{t}), \quad (9)$$

where $\tilde{J}_{\parallel 0}(\tilde{t})$ is the current at $\tilde{\ell} \gg 1$. From (6) we have

$$\tilde{u}_{\text{in}} = \frac{1}{\tilde{B}_0(\tilde{\ell})} \int_0^{\tilde{\ell}} d\tilde{\ell}' \frac{\tilde{B}_0(\tilde{\ell}')}{|\tilde{\nabla}\alpha|^2} \left(\frac{\partial \tilde{J}_{\parallel\text{in}}}{\partial \tilde{t}} + \frac{\tilde{J}_{\parallel\text{in}}}{\mathcal{S}} |\tilde{\nabla}\alpha|^2 \right). \quad (10)$$

The inner solution therefore depends on a single unknown function of time, $J_{\parallel 0}(t)$, which we shall determine by matching to the outer solution. We can deduce the value of $J_{\parallel 0}(t)$ at early times by assuming that the forcing-ramp-up time ϵ^{-1} is small compared with the normalized reconnection timescale τ_{rec} , whatever the latter turns out to be (we show how to relax this restriction in Section 3 of the Supplementary Information). In that case, $\Delta\psi$ is unchanged between $\tilde{t} = 0$ and $\epsilon^{-1} \ll \tilde{t} \ll \tau_{\text{rec}}$. At such times, Eqs. (8) and (9) require that

$$\tilde{J}_{\parallel 0}(t) = \mathcal{J}_0 \equiv |\Delta'| \int_{-\infty}^{\infty} d\tilde{\ell} \frac{\tilde{B}_0(\tilde{\ell})}{|\tilde{\nabla}\alpha|^2} \int_{-\infty}^{\tilde{\ell}} d\tilde{\ell}' \lim_{\tilde{t} \rightarrow \infty} \tilde{F}, \quad (11)$$

where $1/|\Delta'| \equiv \int_0^{\infty} d\tilde{\ell} \tilde{B}_0(\tilde{\ell})/|\tilde{\nabla}\alpha|^2$.

MHD case: (ii) Outer region (diffusive). At $\tilde{\ell} \gg 1$, the force \tilde{F} is zero. Because $\epsilon \ll 1$, we also neglect the induction term in Eq. (6) compared with the diffusive one. In this case, \tilde{u}_{out} satisfies a diffusion equation:

$$\frac{\partial \tilde{u}_{\text{out}}}{\partial \tilde{t}} = \frac{\mathcal{S}}{|\tilde{\nabla}\alpha|^2} \frac{\partial^2 \tilde{u}_{\text{out}}}{\partial \tilde{\ell}^2}, \quad |\tilde{\nabla}\alpha|^2 = \Lambda e^{2\tilde{\ell}}, \quad (12)$$

where $\Lambda = \exp[2 \lim_{\tilde{\ell} \rightarrow \infty} (\tilde{\ell}(\tilde{z}) - \tilde{z})]/4$ is a constant to be determined from Eq. (4). Eq. (12) admits a similarity variable $\xi = \Lambda e^{2\tilde{\ell}}/4\mathcal{S}\tilde{t}$. Changing variables from $\tilde{\ell}$ to ξ , Eq. (12) becomes

$$\tilde{t} \frac{\partial \tilde{u}_{\text{out}}(\xi, \tilde{t})}{\partial \tilde{t}} = \xi \frac{\partial^2 \tilde{u}_{\text{out}}(\xi, \tilde{t})}{\partial \xi^2} + (1 + \xi) \frac{\partial \tilde{u}_{\text{out}}(\xi, \tilde{t})}{\partial \xi}, \quad (13)$$

of which the series

$$\tilde{u}_{\text{out}}(\xi, \tilde{t}) = \sum_n \tilde{t}^{p_n} f_n(\xi) \quad (14)$$

is a solution if $f_n(\xi)$ satisfies

$$\xi \frac{d^2 f_n}{d\xi^2} + (1 + \xi) \frac{df_n}{d\xi} - p_n f_n = 0, \quad \forall n. \quad (15)$$

The solutions of Eq. (15) that vanish at $\xi \rightarrow \infty$ are $f_n(\xi) = C_n e^{-\xi} U(1 + p_n, 1, \xi)$, where C_n is a constant and U is Tricomi's confluent hypergeometric function.

MHD case: (iii) Matching solutions, $\tilde{t} \ll \mathcal{S}$. For $\tilde{t} \ll \mathcal{S}$, resistive diffusion of the inner solution [the final term in Eq. (10)] can be neglected. The matching condition is then [from Eqs. (9), (10) and $\tilde{J}_{\parallel\text{out}} = \mathcal{S} \partial \tilde{u}_{\text{out}} / \partial \tilde{\ell}$]

$$\lim_{\tilde{\ell} \rightarrow 0} \tilde{u}_{\text{out}} = \lim_{\tilde{\ell} \rightarrow \infty} \tilde{u}_{\text{in}} = \frac{\mathcal{S}}{|\Delta'|} \frac{d}{dt} \lim_{\tilde{\ell} \rightarrow 0} \frac{\partial \tilde{u}_{\text{out}}}{\partial \tilde{\ell}}. \quad (16)$$

Using standard results for Tricomi's function, we have

$$\lim_{\xi \rightarrow 0} \tilde{u}_{\text{out}} = - \sum_n \frac{C_n \tilde{t}^{p_n} \ln(\Theta_n \xi)}{\Gamma(1 + p_n)}, \quad \Theta_n \equiv e^{2\gamma_E + F(1+n)}, \quad (17)$$

up to $O(\xi)$, where γ_E is the Euler–Mascheroni constant and F is the digamma function. For $\tilde{t} \ll \mathcal{S}$, the logarithm in Eq. (17) is constant and approximately equal to $\ln(\Lambda/4\mathcal{S})$. Eqs. (16) and (17) together require that $p_{n+1} = p_n + 1$, $C_{n+1} = -C_n/\tau_{\text{rec}}$, where

$$\tau_{\text{rec}} = \frac{2\mathcal{S}}{|\Delta'| \ln(4\mathcal{S}/\Lambda)}. \quad (18)$$

Matching to Eq. 11 requires $p_0 = 0$, $C_0 = -\mathcal{J}_0/2\mathcal{S}$. Thus, the outer solution is

$$\tilde{u}_{\text{out}} = -\frac{\mathcal{J}_0}{2\mathcal{S}} \sum_{n=0}^{\infty} (-1)^n e^{-\xi} U(1 + n, 1, \xi) \left(\frac{\tilde{t}}{\tau_{\text{rec}}} \right)^n, \quad (19)$$

$$\tilde{J}_{\parallel\text{out}} = \mathcal{J}_0 \sum_{n=0}^{\infty} (-1)^n \xi e^{-\xi} U(1 + n, 2, \xi) \left(\frac{\tilde{t}}{\tau_{\text{rec}}} \right)^n. \quad (20)$$

The inner $\tilde{J}_{\parallel 0}$ solution is given by Eqs. (9) and (10), with $\tilde{J}_{\parallel 0}$ the $\xi \rightarrow 0$ limit of Eq. (20), i.e.,

$$\tilde{J}_{\parallel 0} = \sum_{n=0}^{\infty} \frac{(-1)^n}{n!} \left(\frac{\tilde{t}}{\tau_{\text{rec}}} \right)^n = \mathcal{J}_0 \exp\left(-\frac{\tilde{t}}{\tau_{\text{rec}}}\right). \quad (21)$$

Eqs. (9), (10), (19), and (20) are as obtained from numerical solution of Eqs. (5) and (6) (see Fig. 2). Qualitatively, the solution for $\tilde{t} \ll \tau_{\text{rec}}$ [the $n = 0$ terms in Eqs. (9) and (10)] is a self-similar spreading with similarity variable ξ . The solution is diffusive, but corresponds to negligible reconnection [see Eq. (22) below] until the current begins to decay at $\tilde{t} \sim \tau_{\text{rec}}$, which is when the propagating front reaches $\tilde{\ell} \sim \ln \mathcal{S}$ (corresponding to $\xi \sim 1$).

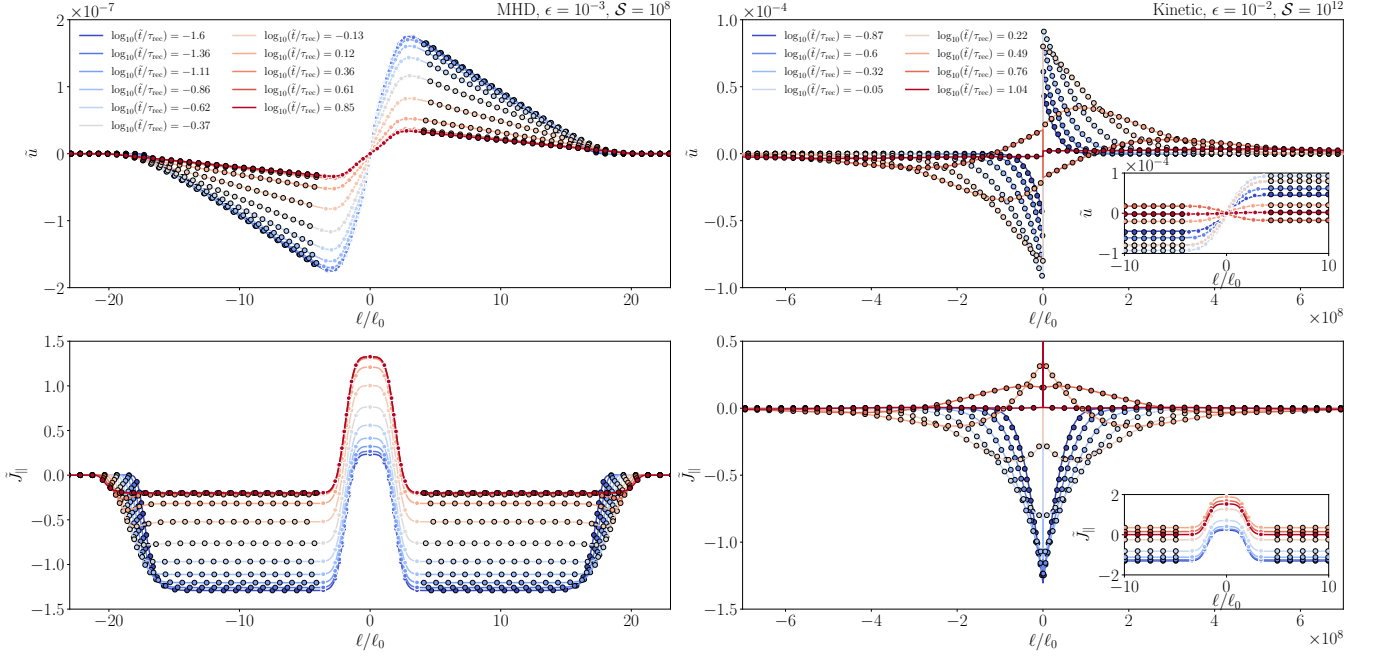


FIG. 2. Evolution of \tilde{u} and \tilde{J}_{\parallel} for $\tilde{t} \sim \tau_{\text{rec}}$. The panels on the left show the MHD case, those on the right show the kinetic case. Solid lines show numerical solutions of Eqs. (5) and (6) obtained with a finite-difference scheme. Dots show the theoretical prediction derived in the main text; dots with black outlines correspond to the outer solution [Eqs. (19) and (20) for the MHD case (corrected for the resistive diffusion of the inner solution, as described in Section 4 of the Supplementary information), Eqs. (25) and (26) for the kinetic case], dots with white outlines correspond to the inner solution [Eqs. (9) and (10)].

MHD case: (iv) Reconnection rate. It follows from Eqs. (8), (9) and (21) that

$$\Delta\psi = \frac{1}{|\Delta'|}(\tilde{J}_{\parallel 0} - \mathcal{J}_0) = -\frac{\mathcal{J}_0}{|\Delta'|} \left[1 - \exp\left(-\frac{\tilde{t}}{\tau_{\text{rec}}}\right) \right] \quad (22)$$

which confirms that τ_{rec} [Eq. (18)] is the reconnection timescale. Eq. (8) correctly reproduces the evolution of $\Delta\psi$ that we obtain numerically (see Fig. 3).

MHD case: (v) Matching solutions, $\tilde{t} \gtrsim \mathcal{S}$. If $\tilde{t} \gtrsim \mathcal{S}$, we cannot neglect \tilde{t} in the logarithm in Eq. (17), nor the final term in Eq. (10). We show how to modify the solution in Section 4 of the Supplementary Information [16]. However, because $\tau_{\text{rec}} \ll \mathcal{S}$ as $\mathcal{S} \rightarrow \infty$, the solution in the preceding sections is the one of primary interest.

Kinetic case: (i) Inner solution (ideal). We neglect inertia in the inner region—because this is the only term in which the kinetic equations are different from the MHD ones, the solutions Eqs. (9) and (10) remain valid in the kinetic case [although $\tilde{J}_{\parallel 0}(\tilde{t})$ is different].

Kinetic case: (ii) Outer solution (diffusive). In the kinetic case, the governing equation for \tilde{u}_{out} is a diffusion equation with constant coefficient \mathcal{S} . We recast it in a form similar to Eq. (23) by changing variables from $\tilde{\ell}$ to a new similarity variable $\xi = \tilde{\ell}/(4\mathcal{S}\tilde{t})^{1/2}$:

$$\frac{\partial \tilde{u}_{\text{out}}}{\partial \tilde{t}} = \mathcal{S} \frac{\partial^2 \tilde{u}_{\text{out}}}{\partial \tilde{\ell}^2} \rightarrow \tilde{t} \frac{\partial \tilde{u}_{\text{out}}}{\partial \tilde{t}} = \frac{1}{4} \frac{\partial^2 \tilde{u}_{\text{out}}}{\partial \xi^2} + \frac{1}{2} \xi \frac{\partial \tilde{u}_{\text{out}}}{\partial \xi}. \quad (23)$$

The solutions of the ordinary differential equation that results from substituting Eq. (14) into Eq. (23) are [cf. (15)] $f_n(\xi) = C_n e^{-\xi^2} U((1+2p_n)/2, 1/2, \xi^2)$.

Kinetic case: (iii) Matching solutions. The matching condition is Eq. (16), as in the MHD case. From the small-argument limit of Tricomi's function, we have

$$\lim_{\xi \rightarrow 0} \tilde{u}_{\text{out}} = \sqrt{\pi} \sum_n C_n \tilde{t}^{p_n} \left[\frac{1}{\Gamma(1+p_n)} - \frac{2\xi}{\Gamma(1/2+p_n)} \right] \quad (24)$$

up to $O(\xi^2)$. Eq. (16) then requires that $p_{n+1} = p_n + 3/2$ and gives the recursion relation $C_{n+1} = -|\Delta'|/\mathcal{S}^{1/2} C_n$, so $C_n = (-|\Delta'|/\mathcal{S}^{1/2})^n C_0$. Matching to the early-time solution (11) gives $p_0 = 1/2$, $C_0 = -\mathcal{J}/\sqrt{\pi}\mathcal{S}^{1/2}$, whence,

$$\tilde{u}_{\text{out}} = -\mathcal{J}_0 \sqrt{\frac{\tilde{t}}{\pi\mathcal{S}}} \sum_{n=0}^{\infty} (-1)^n e^{-\xi^2} U_{n,1/2}(\xi) \left(\frac{\tilde{t}}{\tau_{\text{rec}}} \right)^{3n/2}, \quad (25)$$

$$\tilde{J}_{\parallel \text{out}} = \frac{\mathcal{J}_0}{\sqrt{\pi}} \sum_{n=0}^{\infty} (-1)^n e^{-\xi^2} \xi U_{n,3/2}(\xi) \left(\frac{\tilde{t}}{\tau_{\text{rec}}} \right)^{3n/2}, \quad (26)$$

where

$$\tau_{\text{rec}} = \left(\frac{\mathcal{S}}{|\Delta'|^2} \right)^{1/3}, \quad U_{n,\alpha} \equiv U(1+3n/2, \alpha, \xi^2). \quad (27)$$

These solutions are as we find numerically (see Fig. 2). Qualitatively, the solution for $\tilde{t} \ll \tau_{\text{rec}}$ is a self-similar

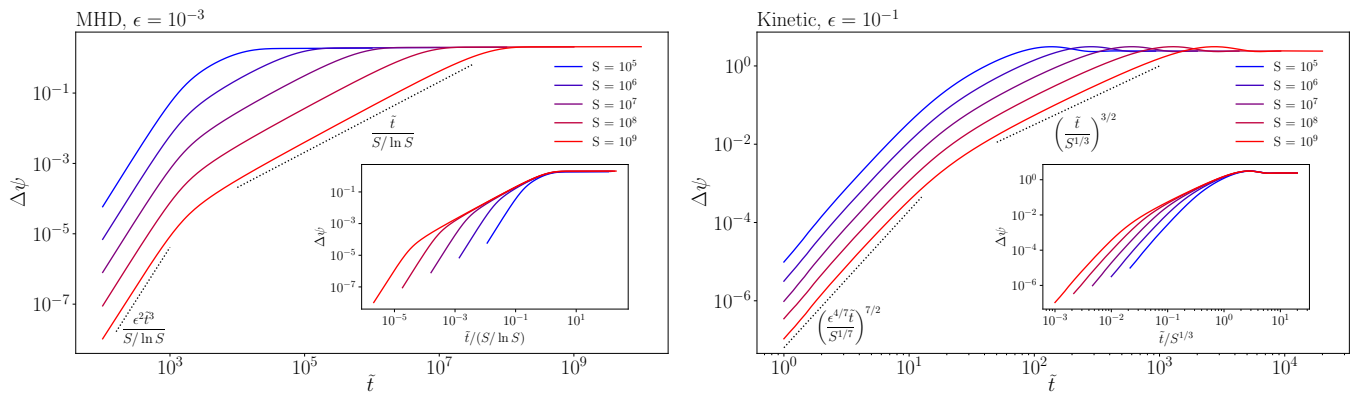


FIG. 3. Evolution of $\Delta\psi$ [Eq. (8)] as a function of time in the MHD (left) and kinetic (right) cases in the numerical solution of Eqs. (5) and (6). At $\tilde{t} \gg 1/\epsilon$, the evolution is as predicted by Eqs. (22) and (28) (see insets, which show time rescaled by the appropriate function of \mathcal{S}). Blue regions indicate $\tilde{t} \lesssim \epsilon^{-1}$, when the force \tilde{F} has not yet reached its final value. The power laws in these regions are derived in Section 3 of the Supplementary Information.

spreading of both \tilde{u}_{out} and $\tilde{J}_{\parallel\text{out}}$, with \tilde{u}_{out} also growing like $\tilde{t}^{1/2}$. Reconnection occurs when the current begins to decay at $\tilde{t} \sim \tau_{\text{rec}}$ [Eq. (28)], which is when the propagating front reaches $\tilde{\ell} \sim \mathcal{S}^{2/3}$.

Kinetic case: (iv) Reconnection rate. Taking the $\xi \rightarrow 0$ limit of Eq. (26), we find [cf. Eq. (22)]

$$\Delta\psi = -\frac{\mathcal{J}_0}{|\Delta\psi|} \left[1 - E_{3/2} \left(-\left(\frac{\tilde{t}}{\tau_{\text{rec}}}\right)^{3/2} \right) \right], \quad (28)$$

where $E_{3/2}(x)$ is the Mittag-Leffler function, a generalization of the exponential function defined by $E_\alpha(x) = \sum_{k=0}^{\infty} x^k / \Gamma(1 + \alpha k)$. Eq. (28) reproduces the numerical evolution of $\Delta\psi$, shown in Fig. 3.

Generalization to other geometries. In the kinetic case, the outer-region diffusion equation (23) is independent of $|\tilde{\nabla}\alpha|(\ell)$. It follows that the solution (28) is valid for *any* magnetic geometry, not just the one described by Eq. (2). By contrast, $|\tilde{\nabla}\alpha|$ does appear in Eq. (13) for the MHD case. For an equilibrium with $|\tilde{\nabla}\alpha| \propto \tilde{\ell}^\delta$ for $\tilde{\ell} \gg 1$, it is readily verified that Eq. (13) has a similarity variable $\xi = \tilde{\ell}/(\mathcal{S}\tilde{t})^{1/2(\delta+1)}$. It follows that [17]

$$\Delta\psi \rightarrow \left(\frac{\tilde{t}}{\tau_{\text{rec}}}\right)^{(\delta+3/2)/(\delta+1)}, \quad \tau_{\text{rec}} \propto \mathcal{S}^{(2\delta+1)/(2\delta+3)} \quad (29)$$

as $\tilde{t}/\tau_{\text{rec}} \rightarrow 0$. Eq. (29) implies that MHD reconnection becomes *slower* as the rate of field-line separation increases (i.e., as δ increases). In the case of linear shear, i.e., $\delta = 1$, for example, $\tau_{\text{rec}} \propto \mathcal{S}^{3/5}$ (as was inevitable because Eqs. (5) and (6) are then isomorphic to the 2D tearing-mode equations [11]). We note that the time taken for the diffusive solutions to develop increases as $\delta \rightarrow 0$; this point will be discussed in a future publication.

Conclusion. We have derived nonlinear solutions for 3D MHD and electron-only reconnection in a sheared magnetic field. In our solutions, reconnection is induced

by diffusing Alfvén- and semi-collisional kinetic-Alfvén-wave packets generated by an external force applied gradually to exponentially separating field lines. Their diffusion changes the connectivity of the global field in a timescale $\propto \mathcal{S}/\ln \mathcal{S}$ and $\propto \mathcal{S}^{1/3}$, respectively. Interestingly, the former timescale reduces if field lines separate more slowly than exponentially with distance [Eq. (29)], while the latter is unchanged.

Acknowledgements. We are grateful to Christopher Ham and Anna Thackray for their collaboration on a related project. We also thank the hosts, organisers and participants of the 2024 Plasma Kinetics Workshop at the Wolfgang Pauli Institute, Vienna, where this work was discussed.

SUPPLEMENTARY INFORMATION

1. Derivation of $|\nabla\alpha|^2$ and $B_0(\ell)$ for the field (2)

From the vector product of $\mathbf{B}_0 = \nabla\psi \times \nabla\alpha$ with $\nabla\psi$,

$$\nabla\alpha = \frac{\mathbf{B}_0 \times \nabla\psi}{|\nabla\psi|^2} + \lambda \nabla\psi, \quad \lambda = - \int_L^\ell \frac{d\ell'}{B_0} \mathcal{I}(\psi, \alpha, \ell'), \quad (30)$$

where $L = L(\alpha, \psi)$ is arbitrary and

$$\mathcal{I}(\psi, \alpha, \ell) = \frac{\mathbf{B}_0 \times \nabla\psi}{|\nabla\psi|^2} \cdot \nabla \times \frac{\mathbf{B}_0 \times \nabla\psi}{|\nabla\psi|^2} \quad (31)$$

is the local shear. It follows from (30) that

$$|\nabla\alpha|^2 = \frac{B_0^2}{|\nabla\psi|^2} + \lambda^2 |\nabla\psi|^2. \quad (32)$$

We proceed to evaluate (32) on the separatrix of the magnetic field (2). Substituting (2) into (31), we obtain

$$\mathcal{I} = - \frac{B_{\text{ext}} \nabla\psi \cdot \nabla |\nabla\psi|^2}{a |\nabla\psi|^4} = - \frac{\ell_0}{a^4} \left(3 + \frac{(a^4 - \chi)}{r^4} \right) \quad (33)$$

where $\chi \equiv \exp(c\psi/aI_0) = (r^2 + a^2)^2 - 4a^2x^2$ and we have used the fact that $|\nabla\chi|^2 = 16r^2\chi$. On the separatrix, where $\chi = a^4$, $\mathcal{I} = -3\ell_0/a^4$, whence

$$\frac{|\nabla\psi|^2}{B_{\text{ext}}^2} = \frac{a^2 r^2}{\ell_0^2}, \quad \frac{B_0^2}{B_{\text{ext}}^2} = 1 + \frac{r^2}{\ell_0^2}, \quad \lambda = \frac{3\ell_0 z}{B_{\text{ext}} a^4}. \quad (34)$$

It remains to determine $r(\ell)$. χ is constant along field lines, so the x and y components of field-line trajectories are $x(r, \chi) = \pm(1/(2a))[\sqrt{((r^2 + a^2)^2 - \chi)}]$ and $y(r, \chi) = \pm(1/(2a))[\sqrt{(\chi - (r^2 - a^2)^2)}]$, respectively. We determine the field-line trajectory in z by integrating $(\partial z/\partial r)_{\psi, \alpha} = (\mathbf{B}_0 \cdot \nabla z)/(\mathbf{B}_0 \cdot \nabla r)$ to yield (in the quadrant $y > 0, x < 0$)

$$\frac{z - a\alpha}{2l_0 a^2} = \frac{\chi}{a^4} \int_{r_0}^r \frac{r dr}{\sqrt{((r^2 + a^2)^2 - \chi)(\chi - (r^2 - a^2)^2)}}. \quad (35)$$

We have fixed the constant of integration in (35) by choosing $\alpha = z/a$ on the semi-infinite surface $y = 0, x < -a$ [see Fig. 1(b)]. In general, Eq. (2) requires $a\alpha = z + g(\chi, r) + f(\chi)$, where $g(\chi, r)$ is the function that generates the constant field $B_{\text{ext}} \hat{z}$ and $f(\chi)$ is arbitrary—our choice corresponds to $f(\chi) = -g(\chi, r_0(\chi))$ with $r_0(\chi) = \sqrt{a^2 + \sqrt{\chi}}$. Evaluating the integral (35) with $\chi = a^4$ and (without loss of generality) $\alpha = 0$, we find

$$r^2 = \frac{2a^2}{\cosh(2z/\ell_0)}. \quad (36)$$

Eqs. (3) and (4) in the main text follow from substitution of (36) into (34) and (32).

2. Derivation of the dynamical equations

We derive Eqs. (5) and (6) in the main text from

$$\frac{\partial}{\partial t} \hat{G}\Phi + \{\Phi, \hat{G}\Phi\} = v_A(\ell) \frac{\partial}{\partial \ell} \nabla_\perp^2 \Psi + \{\Psi, \nabla_\perp^2 \Psi\} \quad (37)$$

and

$$\frac{\partial}{\partial t} \Psi + \{\Phi, \Psi\} = \frac{\partial}{\partial \ell} [v_A(\ell)\Phi] + \eta \nabla_\perp^2 \Psi, \quad (38)$$

where Φ is the streamfunction for the velocity field perpendicular to the local unperturbed magnetic field, $\mathbf{u}_\perp = \mathbf{b}_0 \times \nabla_\perp \Phi$; Ψ is the flux function for the magnetic perturbation, $\delta\mathbf{B}_\perp = \sqrt{4\pi\rho_0} \mathbf{b}_0 \times \nabla_\perp \Psi$; $v_A(\ell) = B_0(\ell)/\sqrt{4\pi\rho_0}$ is the local Alfvén speed associated with the unperturbed field strength $B_0(\ell)$ and density ρ_0 ; the Poisson bracket is

$$\{\Phi, \Psi\} \equiv \mathbf{b}_0 \cdot (\nabla_\perp \Phi \times \nabla_\perp \Psi); \quad (39)$$

\mathbf{b}_0 is the unit vector in the direction of \mathbf{B}_0 [Eq. (44)];

$$\hat{G} = \frac{2}{\rho_i^2} (\hat{\Gamma}_0 - 1), \quad (40)$$

where ρ_i is the ion gyroradius; $\hat{\Gamma}_0$ is the operator whose representation in Fourier space is as multiplication by

$$\Gamma_0(\alpha_i) \equiv I_0(\alpha_i) e^{-\alpha_i}, \quad \alpha_i \equiv \frac{k_\perp^2 \rho_i^2}{2}; \quad (41)$$

and I_0 is the modified Bessel function of the first kind.

Equations (37) and (38) are the semi-collisional limit of the Kinetic Reduced Electron Heating Model (KREHM) of Ref. [8]. They describe the low-frequency (compared with the ion gyrofrequency) anisotropic ($k_\parallel/k_\perp \ll 1$, with k_\parallel and k_\perp the wavenumbers along and across the equilibrium magnetic field, respectively) dynamics of a semi-collisional plasma (collisional electrons but collisionless ions) at small plasma β and large ion-to-electron temperature ratio. For that system, ions have no mean flow and the magnetic field is advected by the $\mathbf{E} \times \mathbf{B}$ motion of electrons. In this study, we focus on the limits of small and large $k_\perp \rho_i$. In the former case, $\hat{\Gamma}_0 = k_\perp^2 \rho_i^2/2$. It follows that $\hat{G} = \nabla_\perp^2$, whence (37) and (38) become the equations of reduced MHD (RMHD) [7]. We refer to this limit as the MHD case in the main text. In the opposite limit $k_\perp \rho_i \gg 1$ (the “kinetic” case in the main text), Γ_0 is exponentially small and $\hat{G} = -2/\rho_i^2$ becomes a multiplication by a constant.

We make the ansatz

$$\Phi(\psi, \alpha, \ell, t) = \bar{\Phi}(\ell, t) e^{in\alpha}, \quad \Psi(\psi, \alpha, \ell, t) = \bar{\Psi}(\ell, t) e^{in\alpha} \quad (42)$$

for the solution of (37) and (38), where $n \gg 1$ enforces narrow localization in the $\nabla\alpha$ direction. Eq. (42) fixes the polarization of the wave to be in the $\mathbf{b}_0 \times \nabla\alpha$ direction; it can be changed by redefining α to incorporate a shift by a function of ψ (which leaves \mathbf{B}_0 unchanged).

The cross product in (39) vanishes after substitution of (42) because perpendicular gradients of Φ and Ψ are both along $\nabla\alpha$. Thus, any solution in the form (42) is a nonlinear solution of (37) and (38). Substituting (42) into (37) and (38), and taking $\mathbf{b}_0 \times \nabla_\perp$ of the result yields

$$G \left(\frac{n^2 |\nabla\alpha|^2 \rho_i^2}{2} \right) \frac{\partial u_\perp}{\partial t} = -n^2 v_A^2 \frac{\partial}{\partial \ell} (|\nabla\alpha|^2 \delta B_\perp), \quad (43)$$

$$\frac{\partial \delta B_\perp}{\partial t} + \eta n^2 |\nabla\alpha|^2 \delta B_\perp = \frac{1}{B_0} \frac{\partial (B_0 u_\perp)}{\partial \ell}, \quad (44)$$

where we have defined u_\perp and δB_\perp such that

$$\delta \mathbf{u}_\perp = u_\perp(\psi, \alpha, \ell, t) e^{in\alpha} \mathbf{b}_0 \times \nabla\alpha, \quad (45)$$

$$\delta \mathbf{B}_\perp = \delta B_\perp(\psi, \alpha, \ell, t) B_0 e^{in\alpha} \mathbf{b}_0 \times \nabla\alpha, \quad (46)$$

and G is the function satisfying $\hat{G}\Phi = G\Phi$, given by

$$G \left(\frac{n^2 |\nabla\alpha|^2 \rho_i^2}{2} \right) = \frac{2}{\rho_i^2} \left[\Gamma_0 \left(\frac{n^2 |\nabla\alpha|^2 \rho_i^2}{2} \right) - 1 \right] \\ \rightarrow \begin{cases} -n^2 |\nabla\alpha|^2 & \text{as } n^2 |\nabla\alpha|^2 \rho_i^2 / 2 \rightarrow 0, \\ -2/\rho_i^2 & \text{as } n^2 |\nabla\alpha|^2 \rho_i^2 / 2 \rightarrow \infty. \end{cases} \quad (47)$$

Eqs. (43) and (44) are identical to Eqs. (5) and (6) after normalizing all variables as described in the main text and appending to them the forcing term in Eq. (5).

3. Evolution of $\Delta\psi$ at $\epsilon\tilde{t} \sim 1$.

At early times $\epsilon\tilde{t} \sim 1$, Eq. (16) is revised to

$$\lim_{\tilde{\ell} \rightarrow 0} \tilde{u}_{\text{out}} = -\frac{\mathcal{J}_0}{|\Delta'|} 2\epsilon^2 \tilde{t} e^{-\epsilon^2 \tilde{t}^2} + \frac{\mathcal{S}}{|\Delta'|} \frac{d}{d\tilde{t}} \lim_{\tilde{\ell} \rightarrow 0} \frac{\partial \tilde{u}_{\text{out}}}{\partial \tilde{\ell}}. \quad (48)$$

Substituting Eq. (9) into Eq. (8), we have that

$$\Delta\psi = \frac{1}{|\Delta'|} \left[J_{\parallel 0}(\tilde{t}) - \mathcal{J}_0(1 - e^{-\epsilon^2 \tilde{t}^2}) \right], \quad (49)$$

where we have taken $\tilde{F} = (1 - e^{-\epsilon^2 \tilde{t}^2}) \tilde{f}(\ell)$, for some function $\tilde{f}(\ell)$ ($F_0 \tilde{\ell}^3 e^{-\ell^2}$ in the plots shown in the main text).

MHD case: Substituting (17) into (48), we find that $p_n = n$ for integers $n \geq 0$, and the C_n are determined by

$$C_{2n+3} = \frac{C_{2n+1}}{\tau_{\text{rec}}^2} + g_n \frac{\mathcal{J}_0 \epsilon^{2+2n}}{\tau_{\text{rec}} \mathcal{S}}, \quad C_{2n+1} = -\frac{C_{2n}}{\tau_{\text{rec}}}, \quad (50)$$

where $g_n = (-1)^n \Gamma(2 + 2n) / \Gamma(1 + n)$. Solving Eq. (50) for the first few C_n and substituting $J_{\parallel 0}(\tilde{t}) = -2\mathcal{S} \sum_n C_n \tilde{t}^n / \Gamma(1 + p_n)$ into Eq. (49), we find

$$\Delta\psi = -\frac{\mathcal{J}_0}{|\Delta'|} \left[\frac{\epsilon^2 \tilde{t}^3}{3\tau_{\text{rec}}} - \frac{\epsilon^2 \tilde{t}^4}{12\tau_{\text{rec}}^2} - \frac{\epsilon^2 \tilde{t}^5}{60\tau_{\text{rec}}^3} (6\tau_{\text{rec}}^2 \epsilon^2 - 1) \right] + O(\tilde{t}^6). \quad (51)$$

Thus, as $\tilde{t} \rightarrow 0$, $\Delta\psi \propto \epsilon^2 \tilde{t}^3 / \tau_{\text{rec}}$, which is the scaling observed in Fig. 3. This persists until either $\tilde{t} \sim \tau_{\text{rec}}$ (at which point the second term in (51) becomes important) or $\epsilon\tilde{t} \sim 1$ (when the third term does).

Kinetic case: Substituting (24) into (48), we find that $p_n = n/2$ for integers $n \geq 0$, and the coefficients C_n are determined by the relations

$$C_{4n+5} = -\frac{C_{4n+2}}{\tau_{\text{rec}}^{3/2}} - \frac{2g_n \mathcal{J}_0 2\epsilon^{2+2n}}{\sqrt{\pi} \tau_{\text{rec}}^{3/2} |\Delta'|}, \quad C_{m+3} = -\frac{C_m}{\tau_{\text{rec}}^{3/2}} \quad (52)$$

for all n and all $m \neq 2 + 4n$. Solving Eq. (52) for the first few C_n and substituting into Eq. (49) $J_{\parallel 0}(\tilde{t}) = -\sqrt{\pi} \mathcal{S} / \tilde{t} \sum_n C_n \tilde{t}^{p_n} / \Gamma(1/2 + p_n)$, we find

$$\Delta\psi = -\frac{\mathcal{J}_0 \epsilon^2}{|\Delta'| \tau_{\text{rec}}^{3/2}} \left[\frac{2\tilde{t}^{7/2}}{\Gamma(9/2)} - \frac{\tilde{t}^5}{60\tau_{\text{rec}}^{3/2}} - \frac{12\epsilon^2 \tilde{t}^{11/2}}{\Gamma(13/2)} \right] + O(\tilde{t}^6). \quad (53)$$

As $\tilde{t} \rightarrow 0$, $\Delta\psi \propto \epsilon^2 \tilde{t}^{7/2} / \tau_{\text{rec}}^{3/2}$, as in Fig. 3. As in the MHD case (51), this scaling persists until either $\tilde{t} \sim \tau_{\text{rec}}$ or $\epsilon\tilde{t} \sim 1$.

4. MHD solution for $\tilde{t} \sim \mathcal{S}$

Including the resistive term in (10), Eq. (16) becomes (at $\epsilon^{-1} \ll \tilde{t}$) [using Eq. (9) and $\tilde{J}_{\parallel \text{out}} = \mathcal{S} \partial \tilde{u}_{\text{out}} / \partial \tilde{\ell}$],

$$\lim_{\tilde{\ell} \rightarrow 0} \tilde{u}_{\text{out}} = \frac{\mathcal{S}}{|\Delta'|} \frac{d}{d\tilde{t}} \lim_{\tilde{\ell} \rightarrow 0} \frac{\partial \tilde{u}_{\text{out}}}{\partial \tilde{\ell}} + \tilde{u}_{FS} + \zeta(\tilde{\ell}) \lim_{\tilde{\ell} \rightarrow 0} \frac{\partial \tilde{u}_{\text{out}}}{\partial \tilde{\ell}} \quad (54)$$

where $\zeta(\tilde{\ell}) \equiv \tilde{B}_0(\tilde{\ell})^{-1} \int_0^{\tilde{\ell}} d\tilde{\ell}' \tilde{B}_0(\tilde{\ell}')$ and

$$\tilde{u}_{FS} \equiv -\frac{1}{\mathcal{S}} \int_0^\infty d\tilde{\ell}' \tilde{B}_0(\tilde{\ell}') \int_{-\infty}^{\tilde{\ell}'} d\tilde{\ell}'' F(\tilde{\ell}''). \quad (55)$$

Substituting Eq. (17) into Eq. (54) yields

$$\sum_n \frac{C_n \tilde{t}^{p_n} (\ln(4\mathcal{S} e^{2\zeta_0} / \Theta_n \Lambda) + \ln \tilde{t})}{\Gamma(1 + p_n)} \\ = \tilde{u}_{FS} - \frac{\mathcal{S}}{|\Delta'|} \sum_n \frac{2C_n p_n \tilde{t}^{p_n - 1}}{\Gamma(1 + p_n)}, \quad (56)$$

where $\zeta_0 = \lim_{\tilde{\ell} \rightarrow \infty} [\int_0^{\tilde{\ell}} d\tilde{\ell}' \tilde{B}_0(\tilde{\ell}') - \tilde{\ell}]$. Expanding around $\tilde{t} = \tilde{t}_0$ for some arbitrary $\tilde{t}_0 > 0$, we obtain

$$\sum_n \bar{C}_n \tau_0 (1 + \delta\bar{\tau})^{n+1} [\ln(\bar{\mathcal{S}} \tau_0 / \Theta_n) + \ln(1 + \delta\bar{\tau})] \\ = \tilde{u}_{FS} \tau_0 (1 + \delta\bar{\tau}) - \sum_n \bar{C}_n n (1 + \delta\bar{\tau})^n, \quad (57)$$

where for convenience we have defined $\tau = \tilde{t} / (2\mathcal{S} / |\Delta'|)$, $\tau_0 = \tilde{t}_0 / (2\mathcal{S} / |\Delta'|)$, $\delta\bar{\tau} = (\tau - \tau_0) / \tau_0$, $\bar{\mathcal{S}} = 8\mathcal{S}^2 e^{2\zeta_0} / \Lambda |\Delta'|$ and $\bar{C}_n = C_n (2\mathcal{S} \tau_0 / |\Delta'|)^n / \Gamma[(n+2)/2]$. To obtain \bar{C}_n , we truncate the sums (at 35 terms) and expand (57) in powers of $\delta\bar{\tau}$. Equating coefficients of each power of $\delta\bar{\tau}$ yields a dense matrix equation for \bar{C}_n , which we solve numerically. The dots in Fig. 2 (left panels) show the corresponding solutions. In constructing these solutions, we choose \tilde{t}_0 to be equal to the time of evaluation.

* dhosking@princeton.edu

- [1] A. H. Boozer, Why fast magnetic reconnection is so prevalent, *J. Plasma Phys.* **84**, 715840102 (2018).
- [2] A. H. Boozer, Fast magnetic reconnection and the ideal evolution of a magnetic field, *Phys. Plasmas* **26**, 042104 (2019).
- [3] T. H. Jensen, R. K. Fisher, C. L. Hsieh, M. A. Mahdavi, V. Vanek, and T. Ohkawa, Confinement of plasma in the Doublet-II Device, *Phys. Rev. Lett.* **34**, 257 (1975).
- [4] T. E. Evans, M. E. Fenstermacher, R. A. Moyer, T. H. Osborne, J. G. Watkins, P. Gohil, I. Joseph, M. J. Schaffer, L. R. Baylor, M. Bécoulet, *et al.*, RMP ELM suppression in DIII-D plasmas with ITER similar shapes and collisionalities, *Nucl. Fusion* **48**, 024002 (2008).
- [5] M. R. Wade, R. Nazikian, J. S. deGrassie, T. E. Evans, N. M. Ferraro, R. A. Moyer, D. M. Orlov, R. J. Buttery, M. E. Fenstermacher, A. M. Garofalo, *et al.*, Advances in the physics understanding of ELM suppression using resonant magnetic perturbations in DIII-D, *Nucl. Fusion* **55**, 023002 (2015).
- [6] D. A. Ryan, C. Ham, A. Kirk, T. Markovic, S. Munaretto, L. Piron, S. Saarelma, W. Suttrop, A. J. Thornton, E. Viezzer, *et al.*, First observation of RMP ELM mitigation on MAST Upgrade, *Plasma Phys. Control. Fusion* **66**, 105003 (2024).
- [7] H. R. Strauss, Nonlinear, three-dimensional magnetohydrodynamics of noncircular tokamaks, *Phys. Fluids* **19**, 134 (1976).
- [8] A. Zocco and A. A. Schekochihin, Reduced fluid-kinetic equations for low-frequency dynamics, magnetic reconnection, and electron heating in low-beta plasmas, *Phys. Plasmas* **18**, 102309 (2011).
- [9] A. A. Schekochihin, S. C. Cowley, W. Dorland, G. W. Hammett, G. G. Howes, E. Quataert, and T. Tatsuno, Astrophysical gyrokinetics: kinetic and fluid turbulent cascades in magnetized weakly collisional plasmas, *Astrophys. J. Suppl.* **182**, 310 (2009).
- [10] We note that the semi-collisional limit (collisionless ions but collisional electrons) means that these waves are immune to Landau damping.
- [11] K. V. Roberts and J. B. Taylor, Gravitational resistive instability of an incompressible plasma in a sheared magnetic field, *Phys. Fluids* **8**, 315 (1965).
- [12] J. W. Connor, R. J. Hastie, and J. B. Taylor, Shear, periodicity, and plasma ballooning modes, *Phys. Rev. Lett.* **40**, 396 (1978).
- [13] J. W. Connor, R. J. Hastie, and T. J. Martin, The stability of resistive ballooning modes in a high temperature plasma, *Plasma Phys. Control. Fusion* **27**, 1509 (1985).
- [14] J. F. Drake and J. Antonsen, T. M., Analytic theory of resistive ballooning modes, *Phys. Fluids* **28**, 544 (1985).
- [15] We require amplitudes to be small compared with the equilibrium scales in order for Eq. (3) to be valid for the perturbed magnetic field.
- [16] Qualitatively, the effect of the modification is that decay of \tilde{u}_{out} and $\tilde{J}_{\parallel\text{out}}$ is arrested at a non-zero value.
- [17] Here we have used the relations $\tilde{J}_{\parallel 0} = \mathcal{S} \lim_{\tilde{t} \rightarrow 0} \partial \tilde{u}_{\text{out}} / \partial \tilde{t}$, $d\tilde{J}_{\parallel 0} / d\tilde{t} = \lim_{\tilde{t} \rightarrow 0} \tilde{u}_{\text{out}}$ and $\lim_{\tilde{t} \rightarrow 0} \tilde{u}_{\text{out}} \propto \tilde{t}^{p_0} f_0(\xi)$ [Eq. (14)], which imply that $d \ln J_{\parallel 0} / d\tilde{t} \propto \mathcal{S}^{1/2(\delta-1)} \tilde{t}^{1/2(\delta+1)}$ as $\tilde{t} \rightarrow 0$.